ISSN 1070-3284, Russian Journal of Coordination Chemistry, 2020, Vol. 46, No. 6, pp. 411–419. © Pleiades Publishing, Ltd., 2020.
Russian Text © The Author(s), 2020, published in Koordinatsionnaya Khimiya, 2020, Vol. 46, No. 6, pp. 366–375.

The authors congratulate Academician I.L. Eremenko with a 70th birthday

Bioisostere Modifications of Cu^{2+} and Zn^{2+} with Pyromucic Acid Anions and N-Donors: Synthesis, Structures, Thermal Properties, and Biological Activity

I. A. Lutsenko[a, *], D. E. Baravikov[b], M. A. Kiskin[a], Yu. V. Nelyubina[a, c], P. V. Primakov[c, d], O. B. Bekker[e], A. V. Khoroshilov[a], A. A. Sidorov[a], and I. L. Eremenko[a, c]

[a] *Kurnakov Institute of General and Inorganic Chemistry, Russian Academy of Sciences, Moscow, 119991 Russia*
[b] *Chuikov School in the South-East of Moscow, Moscow, 109457 Russia*
[c] *Nesmeyanov Institute of Organoelement Compounds, Russian Academy of Sciences, Moscow, 119991 Russia*
[d] *Moscow State University, Moscow, 119991 Russia*
[e] *Vavilov Institute of General Genetics, Russian Academy of Sciences, Moscow, 119991 Russia*
**e-mail: irinalu05@rambler.ru*

Received January 15, 2020; revised January 20, 2020; accepted January 31, 2020

Abstract—Mono- and binuclear complexes $[Cu(Fur)_2(Phen)]$ (**I**), $[Cu_2(Fur)_4(Py)_2]$ (**II**), $[Cu(Fur)_2(Py)_2(H_2O)]$ (**III**), and $[Zn_2(Fur)_4L_2]$ (L = Py (**IV**), Phpy (**V**)) are synthesized using the reactions of copper(II) and zinc(II) acetates with anions of pyromucic acid (2-furancarboxylic acid (HFur)) and N-donor ligands (pyridine (Py), 4-phenylpyridine (Phpy), and 1,10-phenanthroline (Phen)) in acetonitrile. The copper complexes with pyridine are successively formed from the same reaction mixture: at first binuclear complex **II** is formed and then mononuclear complex **III** is formed. All compounds are isolated as single crystals, and their structures are determined by X-ray structure analysis (CIF files CCDC nos. 1974386 (**I**), 1974388 (**II**), 1974389 (**III**), 1974387 (**IV**), and 1974385 (**V**)). The thermal behavior of complexes **II** and **III** is studied by simultaneous thermal analysis. The biological activity in vitro of all complexes is determined toward the nonpathogenic mycobacterial strain *Mycolicibacterium smegmatis*. Complexes **I** and **V** exhibit a high biological activity and are promising for further studies of antitubercular activity.

Keywords: copper(II) and zinc(II) complexes, 2-furancarboxylic acid, structure, differential scanning calorimetry, biological activity

DOI: 10.1134/S1070328420060056

INTRODUCTION

Withstanding to viral and infection diseases is one of the main tasks of the modern medicine. The problem of tuberculosis remains to be the second after AIDS among infection diseases [1]. All ways of developing efficient facilities against *Mycobacterium tuberculosis* (Koch's Bacillus) are blocked because of its phenotypic heterogeneity, enhanced adaptive ability, and the system of genes of natural drug resistance, which provides an anomalous high revival of this pathogen under unfavorable conditions. Possibly, one of the ways of solving this problem is the elucidation of the factors that determine the character of interactions between metal complexes and pathogen cells and are responsible for their bioactive effect. In fact, the bioactivity of the coordination metal compounds toward various pathogens (fungal and bacterial infections, malaria, tuberculosis, and cancer cells) is being actively studied in the recent time [2–10]. Metal ions perform many important functions in bacterial pathogens: they act as necessary cofactors for cellular proteins making them irreplaceable for both structure formation and functioning of the protein and play an important role in the signal transfer and virulence regulation. Therefore, the maintenance of cellular homeostasis of metal ions is decisively significant for the bacterial viability and pathogenic character.

In this work, 2-furancarboxylic acid and zinc(II) and copper(II) ions were chosen as objects of the study. 2-Furancarboxylic acid and its derivatives are acting substances in bactericidal and fungicidal drugs and are often used in biomedical studies, including in the search for drugs against tuberculosis [11–13]. Essential ions of complex forming metals, zinc(II) and

copper(II), are components of the enzymatic systems of living organisms and perform an important role of electron transfer in the respiratory tract [14]. These metal ions react with acid anions to form stable compounds of various structures and compositions.

The purpose of this study is the synthesis of the Cu(II) and Zn(II) complexes with 2-furancarboxylic acid in the presence of the N-donor ligands (1,10-phenanthroline (Phen), pyridine (Py), and 4-phenylpyridine (Phpy)) and determination of their structures, thermal properties, and biological activity in vitro toward *Mycolicibacterium smegmatis*.

EXPERIMENTAL

The complexes were synthesized using commercial reagents and solvents without additional purification: 2-furancarboxylic acid (HFur) (Acros), zinc(II) acetate dihydrate (98%, Acros), copper(II) acetate monohydrate (95%, Acros), pyridine (high-purity grade, Khimmed), 4-phenylpyridine (97%, Aldrich), 1,10-phenanthroline (Alfa Aesar), and acetonitrile (special purity grade, Khimmed).

The IR spectra of the compounds were recorded on a Perkin-Elmer Spectrum 65 FTIR spectrometer using the attenuated total reflectance (ATR) technique in the frequency range from 400 to 4000 cm^{-1}.

Elemental analyses were carried out on a Carlo Erba EA 1108 automated C,H,N analyzer.

The biological activity was determined in the test system *M. smegmatis* mc^2 155 using the paper disc method. The value of the strain growth suppression zone, which was sowed with a lawn on an agar medium around paper discs containing the substance in various concentrations, was detected. The bacteria washed from the Petri dishes with a Tryptone Soya Agar medium M-290 (Himedia) were grown overnight in a Lemco-TW liquid medium (Lab Lemco' Powder, 5 g L^{-1} (Oxoid); Peptone special, 5 g L^{-1} (Oxoid); NaCl, 5 g L^{-1}; Tween-80) at +37°C to the logarithmic mean growth phase at the optical density OD_{600} = 1.5 and mixed with a molten M-290 agar medium in a ratio of 1 : 9 : 10 (culture : Lemco-TW : M-290). The culture was incubated at +37°C for 24 h. The minimum inhibition concentration (MIC) was accepted to be the concentration of the substance at which the growth suppression zone was minimal.

Synthesis of [Cu(Fur)$_2$(1,10-Phen)] (I). Weighed samples of $Cu(OAc)_2 \cdot H_2O$ (0.182 g, 1 mmol) and HFur (0.448 g, 4 mmol) were dissolved in MeCN (40 mL). The obtained suspension was added by Phen (0.200 mg, 1 mmol), and the reaction mixture was kept at 70°C for 3 h. The obtained blue solution was filtered and concentrated to a volume of 20 mL. Dark blue crystals formed one day after were decanted from the mother liquor and dried in an argon flow. The yield of compound **I** was 0.26 g (55%).

For $C_{22}H_{14}N_2O_6Cu$ (**I**)

Anal. calcd., %	C, 56.71	H, 3.03	N, 6.01
Found, %	C, 56.79	H, 2.95	N, 5.92

IR (ν, cm^{-1}): 3137 vw, 3098 w, 3067 vw, 1622 w, 1565 vs, 1516 m, 1483 m, 1473 vs, 1427 m, 1409 w, 1386 vs, 1355 vs, 1254 w, 1225 m, 1187 vs, 1137 m, 1106 w, 1078 m, 1050 vw, 1012 m, 930 m, 889 m, 857 s, 812 vs, 781 vs, 750 s, 738 m, 723 vs, 649 m, 602 m, 564 m, 544 m, 506 w, 469 vs.

Syntheses of [Cu$_2$(Fur)$_4$(Py)$_2$] (II) and [Cu(Fur)$_2$-(Py)$_2$(H$_2$O)] (III). Weighed samples of $Cu(OAc)_2 \cdot H_2O$ (0.182 g, 1 mmol) and HFur (0.448 g, 4 mmol) were dissolved in MeCN (40 mL). The obtained suspension was added by Py (0.3 mL, 4 mmol), and the reaction mixture was kept at 70°C for 3 h. The resulting solution was filtered and concentrated to a volume of 25 mL. Green crystals formed one day after were decanted from the mother liquor and dried in an argon flow. The yield of compound **II** was 0.32 g (44% based on the initial salt). The mother liquor was kept at room temperature during the slow evaporation of the solvent. Blue crystals formed in a day were decanted from the solution and dried in an argon flow. The yield of compound **III** was 0.17 g (37% based on the initial salt).

For $C_{30}H_{22}N_2O_{12}Cu_2$ (**II**)

Anal. calcd., %	C, 49.39	H, 3.04	N, 3.84
Found, %	C, 49.40	H, 3.19	N, 3.88

IR (ν, cm^{-1}): 3125 vw, 1621 vs, 1600 w, 1583 m, 1575 w, 1477 vs, 1447 m, 1414 vs, 1368 m, 1227 m, 1217 vs, 1198 s, 1140 s, 1069 m, 1038 m, 1009 s, 934 m, 883 m, 839 vw, 806 vs, 779 vs, 763 w, 750 vw, 696 vs, 628 m, 616 w, 597 m, 520 vs, 418 s.

For $C_{20}H_{18}N_2O_7Cu$ (**III**)

Anal. calcd., %	C, 52.0	H, 3.93	N, 6.06
Found, %	C, 51.70	H, 3.98	N, 6.02

IR (ν, cm^{-1}): 3223 m, 1599 vs, 1560 m, 1488 w, 1472 s, 1448 s, 1392 s, 1358 s, 1218 m, 1192 s, 1155 w, 1136 w, 1070 s, 1046 m, 1009 s, 952 vw, 930 m, 882 m, 788 vs, 751 s, 695 s, 640 m, 598 w, 577 vw, 474 s, 436 m.

Synthesis of [Zn$_2$(Fur)$_4$(Py)$_2$] (IV). Weighed samples of $Zn(OAc)_2 \cdot 2H_2O$ (0.1 g, 0.46 mmol) and HFur (0.206 g, 1.84 mmol) were dissolved in MeCN (40 mL). The obtained suspension was added by Py (0.15 mL, 4 mmol), and the reaction mixture was kept at 70°C for 3 h. The resulting colorless solution was filtered and concentrated to a volume of 20 mL. Colorless crystals formed in a day were decanted from the

mother liquor and dried in an argon flow. The yield of compound **IV** was 0.42 g (57%).

For $C_{30}H_{22}N_2O_{12}Zn_2$ (**IV**)

Anal. calcd., %	C, 49.14	H, 3.02	N, 3.82
Found, %	C, 49.28	H, 3.24	N, 3.98

IR (ν, cm^{-1}): 3117 vw, 3068 vw, 2973 vw, 2098 vw, 1724 s, 1628 br.m, 1601 br.m, 1583 br.w, 1571 br.w, 1547 vw, 1478 vs, 1452 vw, 1412 vs, 1397 vw, 1366 m, 1263 w, 1226 m, 1187 s, 1137 w, 1119 m, 1072 m, 1047 w, 1008 s, 932 s, 884 m, 834 s, 825 s, 801 s, 776 vs, 748 m, 721 w, 698 w, 681 m, 644 w, 608 s, 591 vs, 529 vs, 518 vs, 492 vw.

Synthesis of $[Zn_2(Fur)_4(Phpy)_2]$ (V). Weighed samples of $Zn(OAc)_2 \cdot 2H_2O$ (0.100 g, 0.46 mmol) and HFur (0.206 g, 1.84 mmol) were dissolved in MeCN (40 mL). The obtained suspension was added by Phpy (0.285 mL, 4 mmol), and the reaction mixture was kept at 70°C for 3 h. The resulting colorless solution was filtered and concentrated to a volume of 20 mL. Colorless crystals formed in a day were decanted from the mother liquor and dried in an argon flow. The yield of compound **V** was 0.48 g (45%).

For $C_{42}H_{30}N_2O_{12}Zn_2$ (**V**)

Anal. calcd., %	C, 57.10	H, 3.75	N, 5.79
Found, %	C, 56.95	H, 3.97	N, 5.61

IR (ν, cm^{-1}): 3144 vw, 3054 vw, 2986 vw, 2931 vw, 2253 vw, 2050 vw, 1639 vs, 1614 m, 1586 m, 1575 m, 1477 vs, 1413 vs, 1396 w, 1368 s, 1229 s, 1192 s, 1139 m, 1080 s, 1047 m, 1025 m, 1012 m, 933 s, 884 s, 843 s, 800 vs, 783 vs, 766 s, 745 w, 730 w, 693 s, 626 vs, 613 m, 593 vs, 562 s, 501 br.vs, 486 br.m, 429 vs, 420 s.

X-ray structure analyses of complexes **I** and **III**–**V** were carried out at 120 K (for complex **II**, at 296 K) on a Bruker Apex II DUO diffractometer (CCD detector, MoK_α, λ = 0.71073 Å, graphite monochromator). The structures were solved using the ShelXT program [15] and refined by full-matrix least squares using the Olex2 program [16] in the anisotropic approximation for non-hydrogen atoms. The hydrogen atoms of OH groups were localized from the difference Fourier synthesis, and positions of other hydrogen atoms were calculated geometrically. All of them were refined in the isotropic approximation by the riding model. The diffuse contribution of the disordered solvent molecules was described by the BYPASS option (a.k.a. SQUEEZE) implemented in the program package [16]. Selected crystallographic data and refinement parameters are presented in Table 1.

The full set of X-ray structure parameters was deposited with the Cambridge Crystallographic Data Centre (CIF files CCDC nos. 1974386 (**I**), 1974388 (**II**), 1974389 (**III**), 1974387 (**IV**), and 1974385 (**V**); deposit@ccdc.cam.uk).

The thermal behavior of compounds **II** and **III** was studied by simultaneous thermal analysis (STA) in an argon atmosphere with the simultaneous detection of thermogravimetry (TG) and differential scanning calorimetry (DSC) curves. The study was conducted on an STA 449 F1 Jupiter instrument (NETZSCH) in aluminum crucibles under a cap with a hole providing a vapor pressure of 1 atm during the thermal decomposition of the samples. The heating rate was 10°C/min to 450°C. The weight of the samples was 10.99 mg (**II**) and 4.12 mg (**III**). The temperature measurement accuracy was ±0.7°C, and the weight change accuracy was $\pm 1 \times 10^{-2}$ mg. The correction file and temperature and sensitivity calibrations for the specified temperature program and heating rate were used when recording the TG and DSC curves. After thermal analysis, the qualitative determination of the chemical composition was carried out and the micromorphology of the residual substance was examined on an NVision 40 scanning electron microscope (Carl Zeiss) equipped with an Oxford X-Max X-ray spectral detector at an accelerating voltage of 1 and 20 kV, respectively. The magnification ranged from ×3000 to ×300000.

RESULTS AND DISCUSSION

The synthetic task of this study was the preparation of the copper(II) and zinc(II) complexes with Fur^- anions and various sets of N-donor ligands. This strategy was aimed at determining the influence of the N-donor nature on the compositions, structures, and biological activities of the formed compounds. The copper and zinc complexes were synthesized by the reactions of copper and zinc acetates and HFur in a ratio of 1 : 4 followed by the addition of the N-donor. Such a mutual exchange of the acid residues is named the bioisostere modification.[1] A suspension formed at the stage of mixing the metal salt and carboxylic acid gave a solution upon the addition of the ligand and storage of the reaction mixture at 70°C. The crystals of the complexes were isolated from the reaction solutions. Two products were isolated from the reaction mixture of $Cu(OAc)_2 \cdot H_2O$, HFur, and Py. Complex $[Cu_2(Fur)_4(Py)_2]$ (**II**) was formed at the first stage of crystallization, and the subsequent storage of the mother liquor gave the second product: complex $[Cu(Fur)_2(Py)_2(H_2O)]$ (**III**). It can be assumed that complex **III** is formed due to an increase in the pyridine concentration over the content of copper(II) ions as complex **II** precipitates.

All synthesized compounds were isolated as single crystals, which made it possible to determine their crystal structures. Selected bond lengths in complexes **I**–**V** are presented in Table 2.

[1] Bioisostere modifications are structural rearrangements performed via the exchange of atoms by other groups of atoms with gaining, retention, or improvement of the biological properties.

Table 1. Crystallographic parameters and structure refinement parameters for compounds **I–V**

Parameter	Value				
	I	**II**	**III**	**IV**	**V**
FW	465.91	729.60	461.91	733.26	967.56
T, K	120	296	120	120	120
Crystal system	Monoclinic	Monoclinic	Monoclinic	Monoclinic	Monoclinic
Space group	$P2_1/n$	$P2_1/c$	$P2_1$	$P2_1/c$	$P2_1/c$
Crystal size, mm; color	0.2 × 0.1 × 0.1; blue	0.3 × 0.15 × 0.158; green	0.2 × 0.06 × 0.06; dark blue	0.3 × 0.1 × 0.1; colorless	0.2 × 0.2 × 0.1; colorless
a, Å	9.7524(5)	8.6154(7)	5.6787(5)	8.7218(13)	8.0447(2)
b, Å	17.5838(8)	19.3254(14)	21.853(2)	19.369(3)	29.3563(8)
c, Å	10.9894(5)	9.1674(7)	8.3890(7)	9.1026(14)	9.5325(2)
β, deg	99.7370(10)	111.323(2)	108.124(3)	111.838(3)	111.6060(10)
V, Å^3	1857.36(15)	1421.85(19)	989.38(15)	1427.4(4)	2093.04(9)
Z	4	4	2	2	2
ρ_{calc}, g/cm^3	1.666	1.7040	1.550	1.706	1.687
μ, mm^{-1}	1.222	1.568	1.150	1.753	2.846
F(000)	948	742	474	744	1080
Range of data collection over θ, deg	2.208–25.242	2.11–27.99	2.555–27.473	2.103–25.242	3.01–67.87
Ranges of reflection indices	$-12 \le h \le 12$, $-22 \le k \le 19$, $-14 \le l \le 14$	$-12 \le h \le 11$, $0 \le k \le 25$, $0 \le l \le 12$	$-7 \le h \le 7$, $-28 \le k \le 28$, $-10 \le l \le 10$	$-11 \le h \le 11$, $-25 \le k \le 25$, $-12 \le l \le 12$	$-9 \le h \le 9$, $-31 \le k \le 34$, $-10 \le l \le 11$
Number of measured reflections	16683	4305	10866	16208	28170
Number of independent reflections (R_{int})	4062 (0.0562)	3438 (0.0000)	4516 (0.0605)	3441 (0.0678)	3750 (0.0435)
Number of reflections with $I > 2\sigma(I)$	3158	2685	3682	3014	3556
Refinement variables	280	208	279	208	290
GOOF	1.027	1.0140	1.025	1.080	1.079
R factors for $F^2 > 2\sigma(F^2)$	$R_1 = 0.0392$, $wR_2 = 0.0892$	$R_1 = 0.0367$, $wR_2 = 0.0764$	$R_1 = 0.0523$, $wR_2 = 0.0878$	$R_1 = 0.0373$, $wR_2 = 0.0860$	$R_1 = 0.0330$, $wR_2 = 0.0833$
R factors for all reflections	$R_1 = 0.0562$, $wR_2 = 0.0982$	$R_1 = 0.0545$, $wR_2 = 0.0858$	$R_1 = 0.0688$, $wR_2 = 0.0937$	$R_1 = 0.0446$, $wR_2 = 0.0891$	$R_1 = 0.0346$, $wR_2 = 0.0845$
Residual electron density (min/max), e/Å^3	–0.396/ 0.897	–0.5065/0.5596	–0.622/0.466	–0.891/0.678	–0.416/0.479

Table 2. Selected bond lengths for complexes **I**–**V**

Bond	*d*, Å				
	I	**II**	**III**	**IV**	**V**
M–O(Fur)	1.955(2)–1.9719(18)	1.9728(15)–1.9742(19)	1.947(4)–1.960(4)	2.0424(19)–2.0563(15)	2.0198(14)–2.0672(17)
M–O(H_2O)			2.218(4)		
M–N	2.000(2)–2.024(2)	2.168(3)	2.025(5)–2.031(5)	2.041(2)	2.0252(19)

Complex **I** is mononuclear: the copper(II) atom is surrounded by two O atoms of two furanate anions and two atoms of N-chelate Phen molecule (Fig. 1a). Two O atoms of both carboxylate groups form weak contacts with the copper atom (Cu...O 2.497, 2.532 Å). The geometry of the CuO_2N_2 polyhedron corresponds to a distorted square. π–π-Stacking interactions organizing individual molecules into chains with a distance between the cycles of 3.608(3) Å and an angle of 0.00(19)° (Fig. 2) are observed between the phenanthroline cycles of the adjacent molecules of the complex.

Complex **III**, as well as complex **I**, is mononuclear: each copper atom coordinates two O atoms of two Fur^- anions, two N atoms of two pyridine molecules, and the O atom of the water molecule (Fig. 1b). The geometry of the CuO_3N_2 polyhedron corresponds to a square pyramid, whose base is formed by the N and O atoms of the carboxylate groups. As follows from the X-ray structure data (Table 2), mononuclear complexes **I** and **III** contain the strongest bonds between the Cu and O atoms of the acid fragments, which is a result of the anion-cationic interactions. The water molecule coordinated to the copper atom in complex **III** forms hydrogen bonds with the oxygen atoms of the carboxylate anions of the adjacent molecule (2.728(9) Å, 2.744(9) Å; 175(7)°, 169(5)°) to form the 1D polymeric motif (Fig. 3).

Complexes **II**, **IV**, and **V** are binuclear tetracarboxylate-bonded complexes (Fig. 4, Table 2). In these compounds, each metal atom is surrounded by four O atoms of four μ-bridging carboxylate groups and one N atom of the pyridine fragment. The environment of the metal atoms of MO_4N corresponds to a square pyramid with the O atoms in the base. The heterocycles inside the molecule are arranged pairwise in the mutually perpendicular planes (Fig. 5). An analysis of the molecular packing of the complexes in crystals revealed an overlapping of the pyridine and furan cycles of the adjacent molecules. The M–O (Fur^-) bonds in complexes **IV** and **V** are fairly close to each other and somewhat longer than those in complex **II** (Table 2).

The thermal behavior of complexes **II** and **III** was studied by the STA method in an argon atmosphere (with the simultaneous detection of the TG and DSC curves) to 450°C. The differences in the compositions and structures of the complexes resulted in different characters of the thermolysis processes. Complex **II** is thermally stable to 175°C. The compound decomposes in one stage with the single endothermic effect (extreme at 243°C) (Fig. 6a, curves *1*, *2*). A similar character of thermolysis was observed earlier for the zinc(II) pivalate complex [17]. Three main stages are observed on the TG curve of complex **III** (Table 3; Fig. 6b, curve *1*): the first stage in a range of 75–140°C

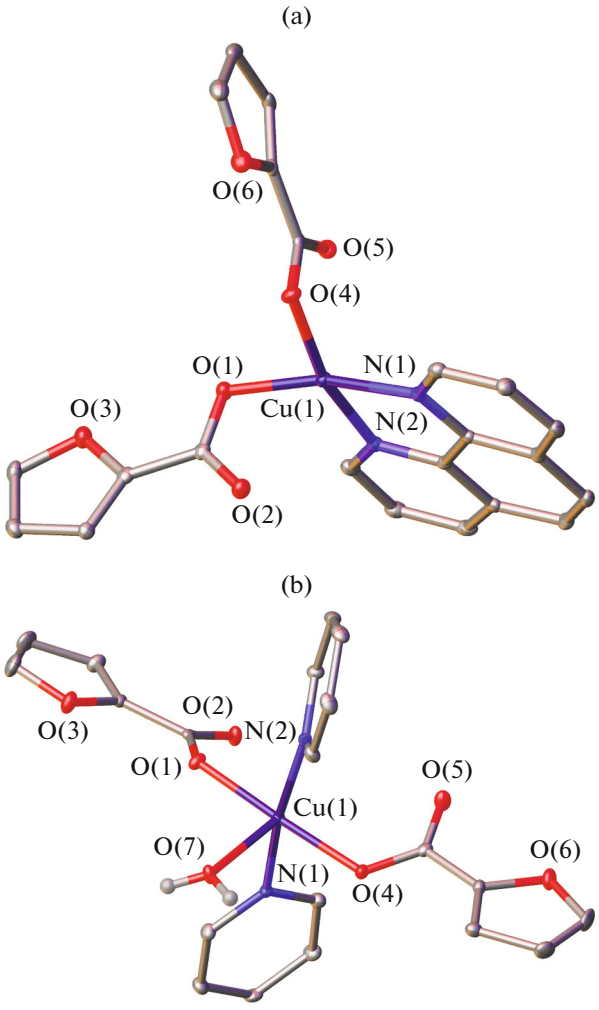

Fig. 1. General views of complexes (a) **I** and (b) **III** in the atomic representation by thermal vibration ellipsoids (p = 50%). The C–H hydrogen atoms are omitted for clarity.

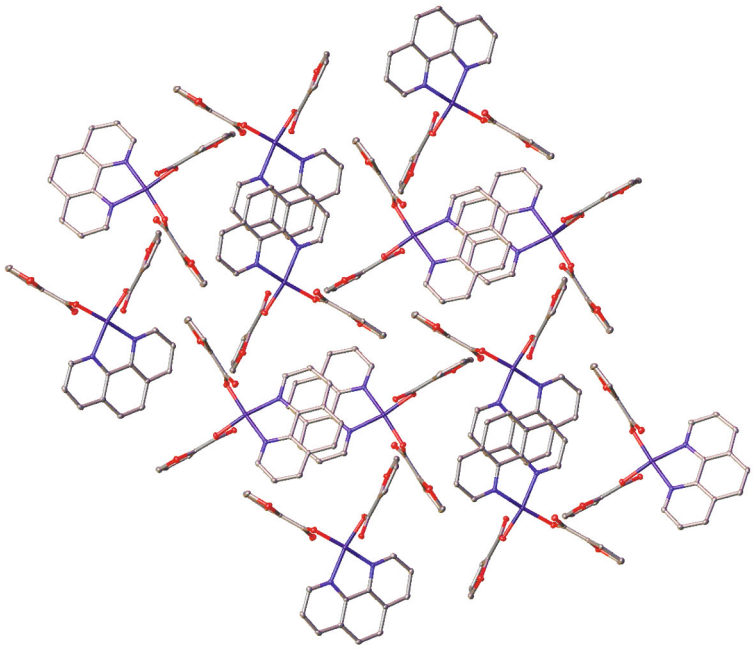

Fig. 2. General view of the packing of complex **I** in the atomic representation by thermal vibration ellipsoids (p = 50%). The C–H hydrogen atoms are omitted for clarity.

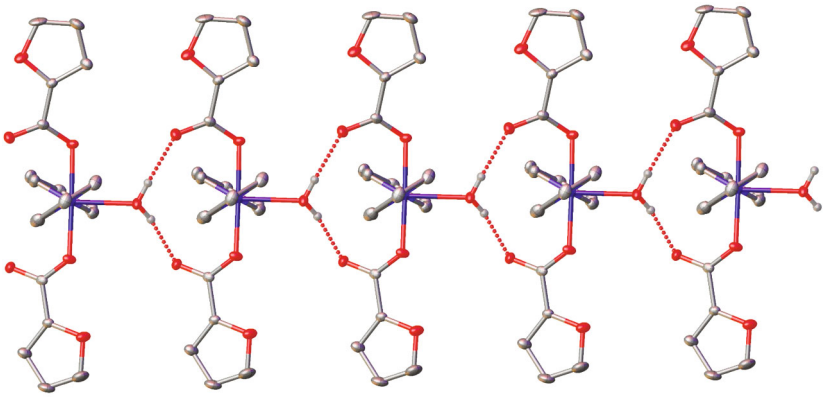

Fig. 3. Formation of the 1D motif in complex **III**. General view of the hydrogen bonds between the molecules of complex **III** in the atomic representation by thermal vibration ellipsoids (p = 50%). The C–H hydrogen atoms are omitted for clarity.

is accompanied by an endothermic effect (extreme at 120°C) and corresponds to the desorption of the coordinated water molecule (T_b = 100°C) and one pyridine molecule (T_b = 115.6°C). The total mass loss at this stage is 20.9%, which completely coincides with the theoretical value. The second and third stages follow each other almost without mass stabilization on the TG curve (Fig. 6b, curve *1*). Stage 2 (Table 3) corresponding to the desorption of the second pyridine molecule ($m_{theor/exp}$ = 17.1/17.4%) transits to the next stage: 2-furancarboxylic acid decarboxylation (200–205°C [18]) and the partial decomposition of the COO^- anion. The DSC curve of complex **III** (Fig. 6b, curve *2*) exhibits the complex endo peak (extreme at 253°C) transformed into the exo peak (extreme at 260°C). Only ~40% weight of 48% of the total mass of the complex falling onto the acid residues are removed to 320°C, and the remained portion eliminates to the end of the process. The residues after the thermolysis of complexes **II** and **III** represent black substances with metallic luster. To determine the final substance (**III**), EDX was carried out and the micromorphology was examined (Fig. 7). The results of the experiments show that the thermolysis product contains Cu (13.58%), O (11.75%), and C (74.67%), which corresponds to the formation of CuO with some carbon content (a low experimental temperature and an inert

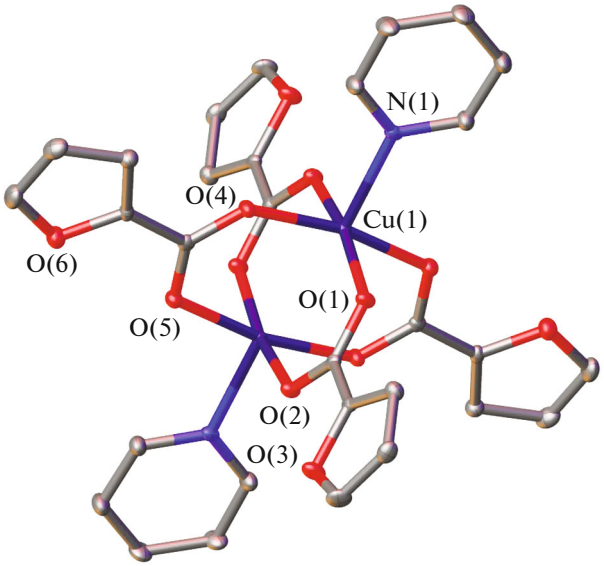

Fig. 4. General view of complex **II** in the atomic representation by thermal vibration ellipsoids ($p = 50\%$). The C–H hydrogen atoms are omitted for clarity, and only the non-carbon atoms in the symmetrically independent part of the molecule are enumerated.

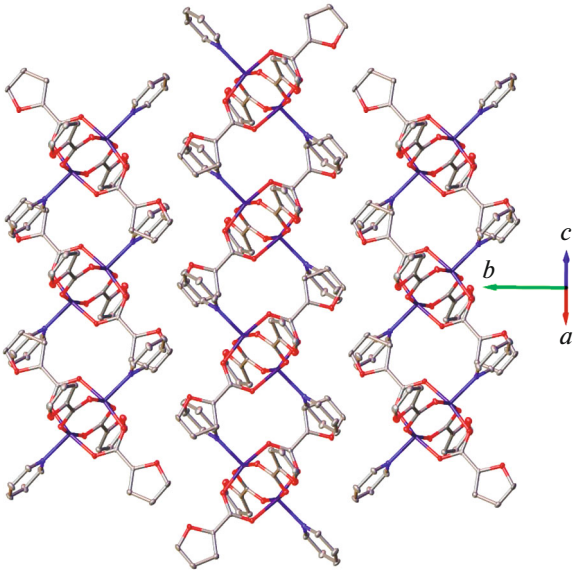

Fig. 5. General view of the packing of complex **II** in the atomic representation by thermal vibration ellipsoids ($p = 50\%$). The C–H hydrogen atoms are omitted for clarity.

atmosphere do not allow carbon to desorb completely). Therefore, the final weight of the residue is somewhat overestimated.

All results obtained on the bioactivity in vitro of the tested compounds were compared with the activity for isoniazid (INH) and rifampicin (RMP) under the given experimental conditions. The N-donor ligands used in the synthesis exhibit no biological activity. The antimicrobial activity of individual HFur toward *M. smegmatis* is insignificant (Table 4). However, an increase in the bioactivity was observed in the metal complex [19]. We conducted experiments on the determination of the bacteriological efficiency of the complexes depending on the ligand and/or complexing metal.

The antibacterial activity of compounds **I**–**V** was determined toward the nonpathogenic strain *M. smegmatis*. It is known that the resistance of mycobacteria to chemotherapeutical agents is related to a low permeability of the mycobacterial cell wall and its unusual structure. *M. smegmatis* are rapidly growing nonpathogenic bacteria and, hence, are used as a model organism for slowly growing bacteria *M. tuberculosis* and for the primary screening of antitubercular drugs [20]. The test system *M. smegmatis* manifests a higher resistance to antibiotics than *M. tuberculosis* and, therefore, the selection criterion is the substance concentration <100 nmol/disc, unlike *M. tuberculosis* [21]. The testing method includes the quantitative estimation of the diameter of the growth suppression zone of the *M. smegmatis* culture grown as a lawn on an agar medium around paper discs impregnated with the tested compounds. The substances were deposited on the discs in various concentrations. The halo diameter (zone of growth inhibition) increased with an increase in the amount of the substance deposited on the disc. The concentration of the substance (μg/disc) at which the minimum visible growth suppression zone is observed is considered to be the MIC. The results on the antibacterial activity in the test system *M. smegmatis* mc^2 155 and its change in time for compounds **I**–**V** are presented in Table 4. As can be seen from the data in Table 4, compounds **II**–**IV** with pyridine as a coligand exhibit no biological activity. When pyridine is replaced by its derivative Phpy in compound **V**, the biological activity of the complex increases and

Table 3. STA data for complexes **II** and **III** (argon atmosphere)

Complex	Stage/ΔT, °C	Δm (TG), %	$T_{endo/exo}$, °C	m_{fin}, %
II	1/125–206	69	243 ± 0.7, 248 ± 0.7	28.7
III	1/75–140	20.9	120 ± 0.7	
	2/140–236	17.5	230 ± 0.7	
	3/236–286	59.1	253 ± 0.7, 260 ± 0.7	2.52

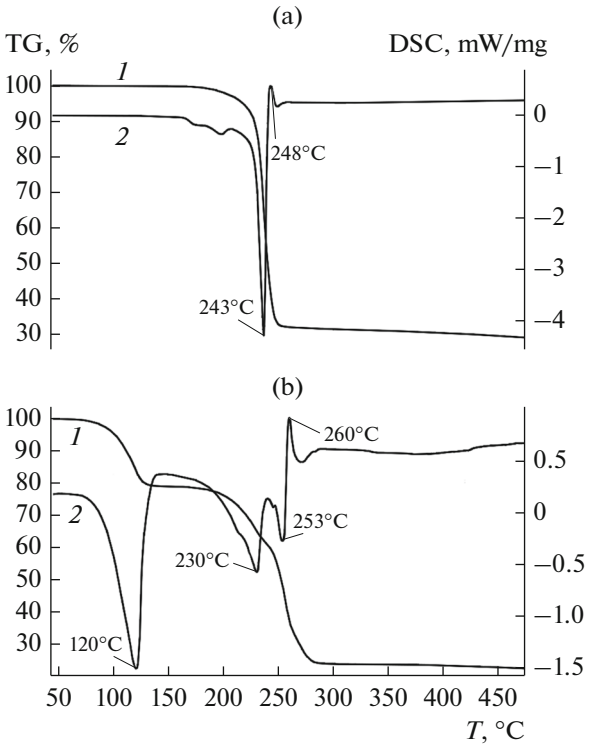

Fig. 6. (*1*) TG and (*2*) DSC curves for complexes (a) **II** and (b) **III**.

becomes comparable with the activity of isoniazid. The results of using 1,10-phenanthroline as an additional ligand in copper complex **I** were unexpected: its biological activity turned out to be five times higher than that of RMP and approximately 12.5 times higher than that of INH.

Thus, it was shown that copper(II) and zinc(II) ions with 2-furancarboxylic acid anions formed the binuclear complexes with the monodentate N-donor ligands, pyridine or 2-phenylpyridine. The mononuclear copper(II) complex with pyridine is formed as the second reaction product, most likely, against the background of an increase in the Py concentration in the reaction mixture. The use of chelating 1,10-phenanthroline in the reaction with copper(II) leads to the formation of the mononuclear complex. Complexes **I** and **II** are the most perspective compounds among the samples tested to biological activity in vitro toward *M. smegmatis*, and their bioefficiency is comparable with (complex **V**) or significantly higher (complex **I**) than those of rifampicin and isoniazid.

ACKNOWLEDGMENTS

The authors are grateful to Kh. Erov for performing SEM and EDX experiments.

The X-ray structure studies were supported by the Ministry of Science and Higher Education of the Russian Federation using the scientific equipment of the Center of Investigation of Structure of Molecules at the Nesmeyanov Institute of Organoelement Compounds (Russian Academy of Sciences). Elemental analysis, STA, and IR spectroscopy were carried out using the equipment of the Center for Collective Use "Physical Methods of Investigation" at the Kurnakov Institute of General and Inorganic Chemistry (Russian Academy of Sciences) supported by the state task of the Kurnakov Institute of General and Inorganic Chemistry (Russian Academy of Sciences) in the sphere of basic research.

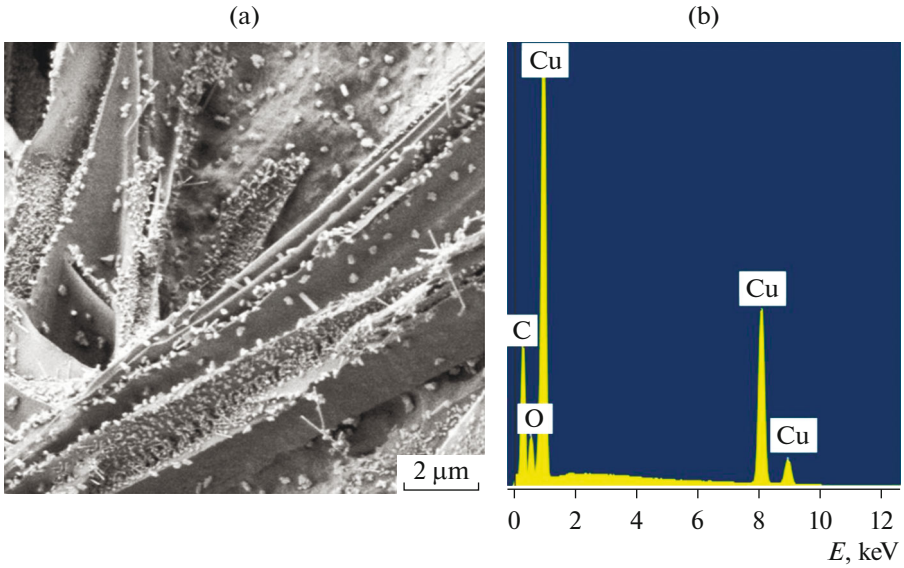

Fig. 7. (a, ×10 000) Image of the micromorphology and (b) the EDX spectrum of the residual substance after the thermolysis of complex **III**.

Table 4. Data on the antibacterial activity toward *Mycolicibacterium smegmatis*

Compound	MIC, μg/disc	Inhibition zone, mm	
	24 h	24 h	120 h
I	2	7 (transparent)*	7 (transparent)
II	146	7 (turbid)**	7 (turbid)
III	153	7 (turbid)	7 (turbid)
IV	366	6.5 (transparent)	6.5 (transparent)
V	41	6.5 (transparent)	6.5 (transparent)
HFur	112		
INH	25	7 (turbid)	6.5 (turbid)
RMP	41	6.5 (transparent)	6.5 (transparent)

* The inhibition of culture growth is not overgrown within the indicated time. ** The inhibition of culture growth of bacteria initially formed after several hours of growth begins to become overgrown over the whole surface of the zone.

FUNDING

This work was supported by the state task of the Kurnakov Institute of General and Inorganic Chemistry (Russian Academy of Sciences) in the sphere of basic research and by the programs of the Russian Academy of Sciences.

CONFLICT OF INTEREST

The authors declare that they have no conflicts of interest.

REFERENCES

1. *WHO Global Tuberculosis Report 2018*, Geneva: World Health Organization, 2018.
2. Honsa, E.S., Johnson, M.D.L., and Rosch, J.W., *Front. Cell. Infect. Microbiol.*, 2013, vol. 3, p. 92.
3. Nagababu, P., Naveena, J., Latha, L., et al., *Can. J. Microbiol.*, 2006, vol. 52, p. 1247.
4. Phopin, K., Sinthupoom, N., Treeratanapiboon, L., et al., *EXCLI J.*, 2016, vol. 15, p. 144.
5. Rojas, S., Devic, T., and Horcajadac, P., *J. Mater. Chem.*, 2017, vol. 5, p. 2560.
6. Anacona, J.R., Bravo, A., and Lopez, M.E., *Lat. Am. J. Pharm.*, 2012, vol. 31, p. 27.
7. Djoko, K.Y., Goytia, M.M., Donnelly, P.S., et al., *Antimicrob. Agents Chemoter.*, 2015, vol. 59, p. 6444.
8. Tumer, M., Koksal, H., and Serin, S., *Transition Met. Chem.*, 1999, vol. 24, p. 13.
9. Bello-Vieda, N.J., Pastrana, H.F., and Garavito, M.F., *Molecules*, 2018, vol. 23, p. 361.
10. Patel, M.N., Parmar, P.A., and Gandhi, D.S., *J. Enzyme Inhib. Med. Chem.*, 2010, vol. 26, p. 188.
11. Sriram, D., Yogeeswari, P., Vyas, D.R.K., et al., *Bioorgan. Med. Chem. Lett.*, 2010, vol. 20, p. 4313.
12. Elsaman, T., Suliman, M., and Mohamed, M., *Bioorgan. Chem.*, 2019, vol. 88, p. 102969.
13. Stüve, P., Minarrieta, L., and Erdmann, H., *Front. Immunol.*, 2018, vol. 9, p. 495.
14. Ovchinnikov, Yu.A., *Bioorganicheskaya khimiya* (Bioorganic Chemistry), Moscow: Prosveshchenie, 1987.
15. Sheldrick, G.M., *Acta Crystallogr., Sect. A: Found. Adv.*, 2015, vol. 71, p. 3.
16. Dolomanov, O.V., Bourhis, L.J., Gildea, R.J., et al., *J. Appl. Crystallogr.*, 2009, vol. 42, p. 339.
17. Lutsenko, I.A., Kiskin, I.A., Efimov, N.N., et al., *Polyhedron*, 2017, vol. 137, p. 165.
18. Wilson, W.C., *Org. Synth.*, 1927, vol. 7, p. 40.
19. Melnic, S., Prodius, D., Stoeckli-Evans, H., et al., *Eur. J. Med. Chem.*, 2010, vol. 45, p. 1465.
20. Ramon-García, S., Ng, C., Anderson, H., et al., *Antimikrob. Agents Chem.*, 2011, vol. 8, p. 3861.
21. Bekker, O.B., Sokolov, D.N., Luzina, O.A., et al., *Med. Chem. Res.*, 2015, vol. 24, p. 2926.

Translated by E. Yablonskaya